Natural Gas Flow Solvers Using Convex Relaxation

Manish Kumar Singh , *Student Member, IEEE*, and Vassilis Kekatos , *Senior Member, IEEE*

Abstract—The vast infrastructure development, gas flow (GF) dynamics, and complex interdependence of gas with electric power networks call for advanced computational tools. Solving the equations relating gas injections to pressures and pipeline flows lies at the heart of natural gas network (NGN) operation, yet existing solvers that require careful initialization and uniqueness has been an open question. In this context, this article considers the nonlinear steady-state version of the GF problem. It first establishes that the solution to the GF problem is unique under arbitrary NGN topologies, compressor types, and sets of specifications. For GF setups where pressure is specified on a single (reference) node and compressors do not appear in cycles, the GF task is posed as n convex minimization. To handle more general setups, a GF solver relying on a mixed-integer quadratically constrained quadratic program (MI-QCQP) is also devised. This solver can be used for any GF setup at any NGN. It introduces binary variables to capture flow directions, relaxes the pressure drop equations to quadratic inequality constraints, and uses a carefully selected objective to promote the exactness of this relaxation. The relaxation is probably exact in NGNs with nonoverlapping cycles and a single fixed-pressure node. The solver handles efficiently the involved bilinear terms through McCormick linearization. Numerical tests validate our claims, demonstrate that the MI-QCQP solver scales well, and that the relaxation is exact even when the sufficient conditions are violated, such as in NGNs with overlapping cycles and multiple fixed-pressure nodes.

Index Terms—Convex relaxation, energy function minimization, gas flow (GF) equations, McCormick linearization, uniqueness.

I. INTRODUCTION

NATURAL gas has served as a critical energy source for decades, mainly for heating and electric power generation [1]. Thanks to the higher ramping capabilities of gas-fired generators, electric power system operators could achieve higher penetration of uncertain and intermittent renewable generation. In addition, the discovery of substantial new supplies of natural gas in the U.S. has led to a new thrust in the development of gas-centered technologies and analytical tools [2].

Natural gas produced at gas pits and refineries is primarily transported to customer locations via a continent-wide network of pipelines [1]. The safe, reliable, and economical transportation of gas across these networks is ensured by gas system operators [3]. Considering the scale of natural gas networks (NGNs), and their coupling with electric power grids, a plethora of analytical and computational challenges can be envisaged. Stand-alone and gas-electric coupled versions of network expansion planning, optimal scheduling, least-cost procurement, and security analysis are examples of problems that have gained increasing research interest; see [3]–[7]. These problems aim at optimizing varying objectives while respecting network limitations and gas flow (GF) physics.

The flow of natural gas on pipelines is governed by partial differential equations, which under steady-state assumptions, yield nonlinear equations relating pressures and GFs [8]. These equations reveal that the pressure drops along a pipe in the direction of flow due to friction. However, minimum pressure needs to be maintained at consumer nodes to satisfy gas contracts. Therefore, compressors are placed on selected pipelines to increase the pressure at their output based on a typically multiplicative [1], and rarely additive law [9]. Operators need to solve the set of nonlinear equations governing GF in an NGN [10]: For each node, the operator fixes the gas pressure or gas injection rate to specified values. Given also the compression ratios, the GF task aims at finding the injections and pressures at all nodes, as well as the GFs on all pipes. While solving the GF task is central for numerous NGN operations, it is hard to do so even under steady-state and balanced conditions for nontree networks [1].

The GF task is usually handled by the Newton–Raphson (NR)-based solvers. However, their convergence can be sensitive to initialization [11]. A semidefinite program (SDP)-based GF solver attaining a higher success probability than the NR scheme is developed in [10]. Nevertheless, the SDP-based solver fails to solve the GF problem if the network state is far from the states considered in designing the solver. The necessity of proper initialization may be avoided for simpler networks without compressors as the flows and pressures may be found as optimal primal–dual solutions of a convex minimization [12]. Nevertheless, for practical meshed NGNs with compressors, an initialization-independent GF solver is still a research pursuit [8]. Setting scalability aside, if one uses a nonlinear solver for the GF task, the uniqueness of a solution becomes critical.

Papers [9] and [13] prove the uniqueness of a GF solution for NGNs with *additive* compressors.

The contribution of this work is on four fronts. First, Section III establishes that the nonlinear steady-state GF equations enjoy a unique solution even with multiplicative compressors. Building on [8] where uniqueness was shown for GF setups with a single fixed-pressure node, here uniqueness is nontrivially generalized to setups with multiple fixed-pressure nodes. Second, Section IV reformulates the GF task as convex minimization. The obtained solver can handle GF setups with a single fixed-pressure node and compressors not on cycles. Third, Section V expands the analytical claims for the mixed-integer quadratically constrained quadratic program (MI-QCQP) GF solver of [8]. Different from the convex minimization approach, this solver applies to any GF setup and any network. The MI-QCQP solver introduces binary variables to capture flow directions, relaxes the nonlinear GF equations to quadratic inequalities, and uses a carefully selected objective to promote the exactness of the relaxation. The relaxation is provably exact in NGNs with nonoverlapping cycles and a single fixed-pressure node. This significantly extends the claim of [8], where exactness was proved for nonoverlapping cycles and a single fixed-pressure node, but did not allow for compressors in cycles. Having compressors in cycles is a typical arrangement, e.g., when two compressors are connected in parallel. Fourth, to accelerate the MI-QCQP solver, the bilinear terms involved are handled through McCormick linearization. Numerical tests on meshed networks with overlapping cycles and multiple fixed-pressure nodes demonstrate that the MI-QCQP solver finds the unique GF solution even when the assumed sufficient conditions are violated.

II. GF PROBLEM

An NGN can be represented by a directed graph $\mathcal{G} = (\mathcal{N}, \mathcal{P})$. The nodes in the graph represent points of gas supply, demand, or network junctions. The edges are *directed*, and represent pipelines or compressors. Nodes are indexed by $n \in \mathcal{N} := \{1, \ldots, N\}$ and edges by $\ell \in \mathcal{P} := \{1, \ldots, P\}$. Each edge $\ell = (m, n)$ is assigned a direction from the origin node m to the destination node n. If $(m, n) \in \mathcal{P}$, then $(n, m) \notin \mathcal{P}$. For edges corresponding to pipes, this direction is selected arbitrarily. For edges denoting compressors, the direction coincides with the direction of GF since compressors allow only unidirectional flow of gas.

For each node $n \in \mathcal{N}$, let q_n be the gas injection rate from node n to the NGN. By convention, the gas injection q_n is positive for gas source nodes, negative for demand nodes, and zero for junction nodes. Vector $\mathbf{q} \in \mathbb{R}^N$ collects the gas injections across all nodes.

For each edge $\ell = (m, n) \in \mathcal{P}$, let ϕ_ℓ denote its GF rate. By convention, the flow ϕ_ℓ is positive if gas flows from node m to n; and negative, otherwise. The conservation of mass at each node $n \in \mathcal{N}$ dictates that

$$q_n = \sum_{\ell:(n,k)\in\mathcal{P}} \phi_\ell - \sum_{\ell:(k,n)\in\mathcal{P}} \phi_\ell. \tag{1}$$

Under steady-state conditions, the input and output flows on a pipe are identical, and so gas injections are balanced at all times, that is $\sum_{n=1}^N q_n = 0$. Because of this, from the N linear equations in (1), only $(N-1)$ are linearly independent.

The topology of the NGN is captured by its edge-node incidence matrix $\mathbf{A} \in \mathbb{R}^{P \times N}$ with entries

$$A_{\ell,k} := \begin{cases} +1, & k = m \\ -1, & k = n \quad \forall \ell = (m,n) \in \mathcal{P}. \\ 0, & \text{otherwise} \end{cases}$$

Using $\mathbf{A}$, (1) can be compactly expressed as

$$\mathbf{A}^\top \boldsymbol{\phi} = \mathbf{q} \tag{2}$$

where vector $\boldsymbol{\phi} \in \mathbb{R}^P$ stacks the flows ϕ_ℓs along all edges.

For medium- and high-pressure networks, the GFs on pipelines relate to nodal pressures through a set of nonlinear partial differential equations [14], [15]. These equations model the GF dynamics evolving across time and spatially along the pipeline length. However, simplifying assumptions such as ignoring friction, geographical tilt, variations in ambient temperature, and time-varying gas injections, yield the popular steady-state Weymouth equation [16]. If $\psi_n > 0$ denotes the *squared* gas pressure at node $n \in \mathcal{N}$, the pressure drop across pipeline $\ell = (m, n) \in \mathcal{P}$ is given by

$$\psi_m - \psi_n = a_\ell \operatorname{sign}(\phi_\ell)\phi_\ell^2 \tag{3a}$$

$$\psi_n \geq 0 \tag{3b}$$

where parameter $a_\ell > 0$ depends on the physical properties of the pipeline [14]. The function $\operatorname{sign}(x)$ returns $+1$ if $x > 0$; -1 if $x < 0$; and 0 if $x = 0$. The absolute value in (3a) signifies that pressure drops along the direction of flow. In particular, the drop in squared pressures is proportional to the squared flow. We will henceforth refer to ψ_m as pressure rather than squared pressure for brevity. Let us collect all ψ_ns in $\boldsymbol{\psi} \in \mathbb{R}^N$.

To enable the desired flow of gas in an NGN while maintaining pressures within acceptable limits, system operators install compressors at selected pipelines. A pipeline hosting a compressor can be modeled by an ideal compressor that increases the gas pressure, followed by a lossy pipeline that incurs a pressure drop per (3). Apparently, the GFs on the two edges are identical. Let the subset of edges hosting ideal compressors be $\mathcal{P}_a \subset \mathcal{P}$. The edges in $\mathcal{P}_a$ are also referred to as *active pipelines*. The pressures across an active pipeline or compressor $\ell = (m, n) \in \mathcal{P}_a$ are related as

$$\psi_n = \alpha_\ell \psi_m \tag{4a}$$

$$\phi_\ell \geq 0 \tag{4b}$$

where $\alpha_\ell > 0$ is the multiplicative compression factor for compressor ℓ. The unidirectional flow permitted for a compressor is enforced by (4b). The remaining edges, that is, the edges not hosting ideal compressors, constitute the set $\bar{\mathcal{P}}_a := \mathcal{P} \setminus \mathcal{P}_a$ and abide by (3) instead of (4).

In an NGN, a node $r \in \mathcal{N}$ is selected as a reference node. Its pressure is kept fixed. Given ψ_r, if the nodal pressures $\boldsymbol{\psi}$ are known, the flows $\boldsymbol{\phi}$ can be readily computed; and vice versa.

This fact follows immediately from (3) and (4), and is itemized as the following lemma to be used in subsequent arguments.

Lemma 1: Given a reference pressure ψ_r for some $r \in \mathcal{N}$, a pair (ϕ, ψ) satisfying (3) and (4) is uniquely characterized by either ϕ or ψ.

The task of finding ϕ or ψ given a combination of nodal injections and pressures constitutes the GF problem. Oftentimes, gas supply nodes are tuned to maintain a fixed pressure while injecting variable amounts of gas to meet the prescribed pressure under variable demands [3], [17]. Let set $\mathcal{N}_\psi \subset \mathcal{N}$ consist of all nodes with fixed pressures ψ_ns. The reference node r belongs to $\mathcal{N}_\psi$ by definition. Its complement set $\mathcal{N}_q := \mathcal{N} \setminus \mathcal{N}_\psi$ consists of all nodes with fixed injections q_ns. Then, the GF problem can be formally stated now.

Definition 1: Given pressures ψ_n for $n \in \mathcal{N}_\psi$, injections q_n for $n \in \mathcal{N}_q$, the ratios α_ℓ for all compressors $\ell \in \mathcal{P}_a$, and the friction parameters a_ℓ for all lossy pipes $\ell \in \bar{\mathcal{P}}_a$, the GF problem aims at finding the triplet $(\psi, \phi, \mathbf{q})$ satisfying the GF equations (2)–(4).

The GF task involves $N - 1 + P$ equations over $N - 1 + P$ unknowns. It can be posed as the feasibility problem

$$\text{find} \quad \{\mathbf{q}, \phi, \psi\} \qquad (\text{G1})$$
$$\text{s.t.} \quad (2) - (4)$$
$$\text{given } \{q_n\}_{n \in \mathcal{N}_q} \text{ and } \{\psi_n\}_{n \in \mathcal{N}_\psi}.$$

Albeit (2) and (4) are linear, the piecewise quadratic Weymouth equation in (3) is nonconvex while the requirement $\{\phi_\ell \geq 0\}_{\ell \in \mathcal{P}_a}$ further complicates the task. The GF problem is typically solved using the NR's method, yet its convergence depends on the initialization [10], [11], [17]. Commercially available software require careful manual tuning by the gas network operator personnel, though that could be attributed to more detailed models of NGN components.

A popular rendition of the GF problem considers the reference node as the only fixed-pressure node, and all other nodes as fixed-injection nodes [8], [10], [18]. For this rendition, solving the GF problem becomes trivial for a tree network by inverting (2) and using Lemma 1. However, for a meshed NGN, solving the GF problem remains nontrivial. Before developing new GF solvers, the following section establishes that the GF problem in (G1) enjoys a unique solution.

III. UNIQUENESS OF THE GF SOLUTION

We commence with the uniqueness of the GF task under the setup of a single fixed-pressure node, proved in [8, Th. 1].

Theorem 1 (see [8]): If $\mathcal{N}_\psi = \{r\}$ and $\mathcal{N}_q = \mathcal{N} \setminus \{r\}$, the GF problem (G1) has a unique solution, if feasible.

Although the single fixed-pressure setup has been studied widely, setups with multiple fixed-pressure nodes are of critical interest too. This is because gas is typically injected at supplier sites using a controller that maintains constant pressure, rather than a constant rate. To address this need, this section builds on Theorem 1 and establishes the uniqueness of the steady-state GF equations for any $(\mathcal{N}_\psi, \mathcal{N}_q)$ setup. Before doing so, let us briefly review some graph theory preliminaries.

A directed graph $\mathcal{G} = (\mathcal{N}, \mathcal{P})$ is connected if there exists a sequence of adjacent edges between any two nodes. All graphs considered in this work are assumed to be connected. A sequence of adjacent edges between nodes m and n constitutes a *path* $\mathcal{P}_{mn} \subset \mathcal{P}$. The directionality assigned to path $\mathcal{P}_{mn}$ is from m to n. Note that nodes m and n could be connected by multiple paths. Thus, with slight abuse in notation, path $\mathcal{P}_{mn}$ shall represent any arbitrary path between m and n, unless additional conditions are provided. For path $\mathcal{P}_{mn}$, we can define an *indicator vector* $\boldsymbol{\pi}^{mn} \in \{0, 1\}^P$ with ℓth entry

$$\pi_\ell^{mn} := \begin{cases} 0, & \text{if edge } \ell \notin \mathcal{P}_{mn} \\ +1, & \text{if direction of } \ell \text{ agrees with path direction} \\ -1, & \text{otherwise.} \end{cases}$$

A *cycle* is a sequence of adjacent edges (without edge or node repetition) that starts and ends at the same node. With a slight abuse of terminology, the statement "cycle $\mathcal{C}$ *contains* node i" will mean that there exists an edge in $\mathcal{C}$ that is incident to node i. For any cycle $\mathcal{C}$, we can select an arbitrary direction and define its indicator vector $\mathbf{n}^{\mathcal{C}}$ with the ℓth entry

$$n_\ell^{\mathcal{C}} = \begin{cases} 0, & \text{if edge } \ell \notin \mathcal{C} \\ +1, & \text{if direction of } \ell \text{ agrees with cycle direction} \\ -1, & \text{otherwise.} \end{cases}$$

A *tree* is a connected graph with no cycles.

After the graph-theoretic preliminaries, we proceed with the uniqueness of the GF solution for the general GF setup. This proof builds upon the ensuing two lemmas, which are proved in the Appendix.

Lemma 2: Consider path $\mathcal{P}_{mn}$ along edges $\{\ell_1, \ldots, \ell_k\}$ with indicator $\boldsymbol{\pi}^{mn}$. For fixed pressures ψ_m and ψ_n, if flow vectors ϕ and ϕ' with $\phi \neq \phi'$ satisfy (3) and (4), they cannot satisfy

$$\text{sign}(\phi' - \phi) \odot \boldsymbol{\pi}^{mn} > \mathbf{0} \text{ or} \qquad (5a)$$
$$\text{sign}(\phi' - \phi) \odot \boldsymbol{\pi}^{mn} < \mathbf{0} \qquad (5b)$$

where the strict inequalities are understood entrywise.

To get some intuition, suppose that $\boldsymbol{\pi}^{mn}$ takes the value of $+1$ for edges $\{\ell_1, \ldots, \ell_k\}$, and 0 for the remaining edges. According to Lemma 2, if two pairs (ϕ, ψ) and $(\phi,' \psi')$ satisfy (3) and (4) with $\psi_m = \psi'_m$ and $\psi_n = \psi'_n$, then the flows along $\mathcal{P}_{mn}$ cannot uniformly increase from ϕ to ϕ'. In other words, $\phi'_\ell > \phi_\ell$ cannot occur simultaneously for all $\ell \in \mathcal{P}_{mn}$. Flows cannot uniformly decrease either ($\phi'_\ell < \phi_\ell$ for all $\ell \in \mathcal{P}_{mn}$). This holds merely because the pressure drop across a pipe decreases monotonically with GF, and compressors perform a linear scaling [cf., (3) and (4)].

The following lemma describes an interesting effect on how GFs get redistributed when gas injections change.

Lemma 3: Consider two pairs $(\mathbf{q}, \phi)$ and $(\mathbf{q},' \phi')$ satisfying (2). If $\mathbf{q} \neq \mathbf{q}'$, there exists a path $\mathcal{P}_{mn}$ between nodes m and n such that

$$\text{sign}(\phi' - \phi) \odot \boldsymbol{\pi}^{mn} > \mathbf{0} \qquad (6a)$$
$$q'_m > q_m \text{ and } q'_n < q_n \qquad (6b)$$

where $\boldsymbol{\pi}^{mn}$ is the indicator vector for $\mathcal{P}_{mn}$.

Lemma 3 predicates that if gas injections change, there exists a path: 1) along which flows increase uniformly, 2) the source node of the path has increased injection, and 3) the destination node has decreased injection. Lemma 3 has been established in [9] via mathematical induction; see the Appendix for an alternative perhaps more intuitive proof.

Using Theorem 1 and Lemmas 2 and 3, we next prove the uniqueness of the GF task under the general setup.

Theorem 2: The GF problem (G1) has a unique solution, if feasible.

Proof: Proving by contradiction, assume $(\mathbf{q}, \boldsymbol{\phi}, \boldsymbol{\psi})$ and $(\mathbf{q},' \boldsymbol{\phi},' \boldsymbol{\psi}')$ are two distinct solutions of (G1). Consider the GF setup where $|\mathcal{N}_\psi| > 1$; the special case of $|\mathcal{N}_\psi| = 1$ is covered by Theorem 1. If $\mathbf{q} \neq \mathbf{q}'$, then Lemma 3 implies that there exists a path $\mathcal{P}_{mn}$ with indicator vector $\boldsymbol{\pi}^{mn}$ satisfying (6a). Moreover, it holds that $q'_m > q_m$ and $q'_n < q_n$ from (6b). By definition, gas injections q_i are fixed for all nodes $i \in \mathcal{N}_q$. Therefore, nodes m and n cannot be fixed-injection nodes. They have to be fixed-pressure nodes belonging to $\mathcal{N}_\psi$, implying $\psi_m = \psi'_m$ and $\psi_n = \psi_n$. However, with the pressures at nodes m and n fixed, the inequality (6a) contradicts Lemma 2. Hence, the assumption of unequal injections is refuted, implying $\mathbf{q} = \mathbf{q}'$.

Given $\mathbf{q}$ and the reference pressure ψ_r, Theorem 1 asserts that there is unique triplet $(\mathbf{q}, \boldsymbol{\phi}, \boldsymbol{\psi})$ satisfying the GF equations. Since $\mathbf{q} = \mathbf{q}'$, the triplets $(\mathbf{q}, \boldsymbol{\phi}, \boldsymbol{\psi})$ and $(\mathbf{q},' \boldsymbol{\phi},' \boldsymbol{\psi}')$ have to coincide. ∎

The uniqueness claim of Theorem 2 is fairly general since it applies to any NGN topology and any GF setup with a single or multiple fixed-pressure nodes. Having established uniqueness, the following two sections develop a suite of GF solvers: Section IV builds upon an existing convex solver for GF setups with a single fixed-pressure node and no compressors. We develop an unconstrained convex solver as well as an extension that handles compressors on nonoverlapping cycles. Section V adopts a convex relaxation and puts forth an MI-QCQP to handle more general GF setups. The relaxation is provably exact for NGNs with a single fixed-pressure node and nonoverlapping cycles. Nonetheless, numerical tests demonstrate that this MI-QCQP succeeds in finding the unique GF solution in NGNs with multiple fixed-pressure nodes and overlapping cycles as long as compressors are not on overlapping cycles.

IV. ENERGY FUNCTION MINIMIZATION

This section studies the GF task for the special case of $|\mathcal{N}_\psi| = 1$. In an NGN without compressors, the GF task is posed as a convex minimization. The approach can be extended to networks having compressors, but not on cycles.

A. Existing Constrained Energy Function Based GF Solver

Consider solving the GF task for a single fixed-pressure node (the reference node r) and in an NGN without compressors. This task boils down to solving (2) and (3). As shown in [12], the GFs $\boldsymbol{\phi}$ for this GF setup can be found as the minimizer of the convex minimization

$$\min_{\boldsymbol{\phi}} \quad \sum_{\ell \in \mathcal{P}} \frac{a_\ell}{3} |\phi_\ell|^3 \tag{7a}$$

$$\text{s.t.} \quad \mathbf{A}^\top \boldsymbol{\phi} = \mathbf{q}. \tag{7b}$$

This can be readily verified by the first-order optimality conditions of (7). In addition, the pressures $\boldsymbol{\psi}$ can be recovered from the optimal Lagrange multipliers $\boldsymbol{\xi} \in \mathbb{R}^N$ associated with constraint (7b): If $\boldsymbol{\xi}$ is shifted by a constant so that its rth entry equals ψ_r, the remaining entries of this shifted $\boldsymbol{\xi}$ equal $\boldsymbol{\psi}$. Problem (7) can be reformulated as a second-order cone program or tackled via dual decomposition; see [19].

B. Novel Unconstrained Energy Function Based GF Solver

Rather than solving (7) over $\boldsymbol{\phi}$, here we show that one can alternatively find the GF solution via an unconstrained convex minimization over $\boldsymbol{\psi}$ as

$$\min_{\boldsymbol{\psi}} \frac{2}{3} \sum_{(m,n) \in \mathcal{P}} \frac{|\psi_m - \psi_n|^{\frac{3}{2}}}{\sqrt{a_{mn}}} - \mathbf{q}^\top \boldsymbol{\psi}. \tag{8}$$

The convexity of this objective function follows from composition rules. Since this function is convex and differentiable, its unconstrained minimization is equivalent to nulling its gradient vector. Setting the nth entry of this gradient to zero reveals that the minimizer $\boldsymbol{\psi}^*$ of (8) satisfies

$$\sum_{\ell=(m,n) \in \mathcal{P}} \text{sign}(\mathbf{a}_\ell^\top \boldsymbol{\psi}^*) \sqrt{\frac{|\mathbf{a}_\ell^\top \boldsymbol{\psi}^*|}{a_\ell}} = q_n \tag{9}$$

where $\mathbf{a}_\ell^\top$ is the ℓth row of matrix $\mathbf{A}$. Equation (9) is equivalent to eliminating the flows $\boldsymbol{\phi}$ from (2) and (3). As with (7), the ambiguity in pressures could be handled by shifting $\boldsymbol{\psi}^*$ by a constant, so that ψ_r^* agrees with the given pressure at the reference node r. Once pressures $\boldsymbol{\psi}^*$ have been determined, flows can be found using Lemma 1.

Remark 1: In the absence of compressors and when $|\mathcal{N}_\psi| = 1$, the GF task becomes structurally similar to the water flow problem in water distribution networks without pumps [19]. Therefore, the (un)constrained energy function minimization approaches of (7) and (8) apply to the GF and water flow problems alike. For water networks, the decomposition technique of [19] extends (7) and (8) to water network setups with $|\mathcal{N}_\psi| = 1$ and pumps, but pumps cannot lie on cycles. A similar technique can be used to solve the GF problem with compressors not on cycles and $|\mathcal{N}_\psi| = 1$. The only modification needed relates to accounting for the multiplicative pressure law in gas compressors [cf., (4a)] vis-à-vis the additive pressure law of water pumps. Additionally, the decomposition algorithm may be extended to accommodate compressors on nonoverlapping cycles using the flow-recovery procedure provided later as Algorithm 1. Since carrying over this decomposition technique from the water flow to the GF context is straightforward and due to space limitations, it is not presented here.

To handle GF setups with $|\mathcal{N}_\psi| > 1$ and/or NGNs with compressors in loops, a convex relaxation of the Weymouth equation is pursued in the following section.

V. MI-QCQP Relaxation

The minimization approaches of (7) and (8) provide computationally efficient methods to solve the GF problem, but exhibit the following three limitations:
1) they cannot handle multiple fixed-pressure nodes ($|\mathcal{N}_\psi| > 1$);
2) cannot handle compressors on cycles;
3) cannot be extended to optimal GF formulations (e.g., along the lines of [20]).

To overcome these limitations, this section presents an MI-QCQP-based solver that is applicable to any GF setup.

A. Problem Reformulation

The nonconvexity of (G1) is due to the Weymouth equation in (3a). The piecewise quadratic equalities can be relaxed to convex inequality constraints: The pressure drop along a lossy pipe $\ell = (m, n) \in \bar{\mathcal{P}}_a$ is relaxed to the following conditions:
1) $\psi_m - \psi_n \geq a_\ell \phi_\ell^2$ for $\phi_\ell \geq 0$;
2) $\psi_n - \psi_m \geq a_\ell \phi_\ell^2$ for $\phi_\ell \leq 0$.

The two cases can be differentiated using a binary variable x_ℓ capturing the direction of flow ϕ_ℓ. The relaxed pressure drop equations can be compactly written as

$$(2x_\ell - 1)\psi_m + (1 - 2x_\ell)\psi_n \geq a_\ell \phi_\ell^2$$

where $x_\ell = 1$ corresponds to $\phi_\ell \geq 0$, and $x_\ell = 0$ to $\phi_\ell \leq 0$. Despite the relaxation, the bilinear terms $x_\ell \psi_m$ make the aforementioned constraint nonconvex.

The McCormick linearization, popular for approximating multilinear terms by their linear convex envelopes, can be used to handle these bilinear terms [21]. For the special case of bilinear terms involving at least one binary term, the McCormick linearization becomes exact. In fact, it is related to the so-termed big-M trick, but instead of using a single arbitrarily large value for M, it selects different values for M that are specialized per product of variables, which could potentially reduce the running time of mixed-integer programming solvers. Let us briefly review the linearization. Consider the constraint $z_{\ell n} = x_\ell \psi_n$, for which $x_\ell \in \{0, 1\}$ and $\psi_n \in [\underline{\psi}_m, \overline{\psi}_n]$. This constraint can be equivalently expressed via four linear inequalities

$$x_\ell \underline{\psi}_n \leq z_{\ell n} \leq x_\ell \overline{\psi}_n \qquad (10a)$$

$$\psi_n + (x_\ell - 1)\overline{\psi}_n \leq z_{\ell n} \leq \psi_n + (x_\ell - 1)\underline{\psi}_n. \qquad (10b)$$

To verify the exactness, observe that when $x_\ell = 1$, constraint (10b) yields $z_{\ell n} = \psi_n$ and (10a) holds trivially. When $x_\ell = 0$, constraint (10a) enforces $z_{\ell n} = 0$ and (10b) holds trivially. Hence, the constraints in (10) ensure that $z_{\ell n} = x_\ell \psi_n$.

To arrive at an MI-QCQP relaxation of (G1), for all lossy pipes $\ell \in \bar{\mathcal{P}}_a$, the pressure drop constraint of (3a) is replaced by (10) and

$$2z_{\ell m} - 2z_{\ell n} + \psi_n - \psi_m \geq a_\ell \phi_\ell^2 \qquad (11a)$$

$$-\overline{\phi}_\ell(1 - x_\ell) \leq \phi_\ell \leq \overline{\phi}_\ell x_\ell \qquad (11b)$$

where $\overline{\phi}_\ell$ is an upper bound on $|\phi_\ell|$. Constraint (11a) represents the relaxed Weymouth equation, and constraint (11b) defines $x_\ell = \text{sign}(\phi_\ell)$. Similar relaxations have been previously used in [4], [8], and [22]; see Section VI for a detailed comparison.

When solving the GF problem with the Weymouth equations relaxed, the obtained solution is useful only if the relaxation is *exact*, that is when (11a) holds with equality for all ℓ. To render the relaxation provably exact, we convert the feasibility problem (G1) to the MI-QCQP minimization

$$\min \quad r(\boldsymbol{\psi}) \qquad \text{(G2)}$$

$$\text{over} \quad \mathbf{q}, \boldsymbol{\phi}, \boldsymbol{\psi}, \mathbf{x}$$

$$\text{s.t.} \quad (2), (4), (10), (11).$$

The optimization variable $\mathbf{x}$ stacks $\{x_\ell\}_{\ell \in \bar{\mathcal{P}}_a}$, and the objective function is judiciously selected as

$$r(\boldsymbol{\psi}) := \sum_{\substack{(m,n) \in \bar{\mathcal{P}}_a \\ (m,n) \notin \mathcal{S}_\mathcal{C}^a}} |\psi_m - \psi_n|$$

where $\mathcal{S}_\mathcal{C}^a$ is the set of cycles with compressors. These cycles will be also termed as *active cycles*. The cost $r(\boldsymbol{\psi})$ sums up the absolute pressure differences across all lossy pipes not in active cycles. Despite the nonconvexity of (G2) due to the binary variables, this minimization can be handled for moderately sized networks thanks to the advancements in mixed-integer second-order cone solvers. The computational performance of (G2) is further corroborated by our tests. The following section provides network conditions under which the exactness of (G2) can be guaranteed analytically. The tests in Section VII demonstrate numerically that solving (G2) renders the relaxation exact for a much broader class of networks.

For solving tasks such as (G1), NR-based or fixed-point iteration solvers are often preferred as opposed to optimization-based solvers due to computational superiority. However, in addition to guaranteeing convergence irrespective of initialization, problem (G2) can also be used as follows.
1) *Infeasibility:* As a relaxation of (G1), (G2) can be used to screen infeasible GF instances; see Section VII for tests. Such screening is of practical use as suggested in [23].
2) *Initialization:* Problem (G2) could be terminated before reaching optimality to yield initializations for NR solvers, hence combining the benefits of both approaches.
3) *Optimal GF:* The cost of (G2) could be useful as a penalty term that can be added to optimization problems [19], [20]. However, guaranteeing exact relaxation for such problems would need further analysis.

B. Exactness of the Relaxation

The relaxation in (G2) will be analytically shown to be exact under the following network conditions.

Condition 1: The GF setup has a single fixed-pressure node, that is $|\mathcal{N}_\psi| = 1$.

Condition 2: Each edge of the NGN belongs to at most one cycle.

Condition 3: The NGN does not exhibit circulation of gas, that is, $\mathbf{n}^c \odot \boldsymbol{\phi} \not\succeq \mathbf{0}$ and $\mathbf{n}^c \odot \boldsymbol{\phi} \not\preceq \mathbf{0}$ for every cycle $\mathcal{C}$.

Under Condition 1, the nodal injections are fixed *a priori* and the GF task aims at finding the associated (ψ, ϕ). Albeit Definition 1 considered the GF task with multiple fixed-pressure nodes, the setup of a single fixed-pressure node is commonly met; see [8], [10], [18], and [24]. Regarding Condition 2, although it may seem restrictive at the outset, it is satisfied by several practical gas networks [25]. For Condition 3, a circulation occurs when gas flows around a cycle along the same direction. It is easy to verify that gas cannot circulate in a cycle without compressors since the incurred pressure drops along the cycle will all be in the same direction and thus cannot sum up to zero. In cycles with compressors, gas circulation can occur though it would cause an undesirable loss of energy. However, the tests of Section VII demonstrate that the relaxation in (G2) is exact even in setups where the sufficient Conditions 1–3 are all violated.

The next exactness claim applies to the GF setup with known injections. From Lemma 1, we know that solving the GF task is equivalent to finding the correct flows ϕ. The next result provides conditions under which (G2) yields flows ϕ with partially correct entries. An algorithm to retrieve the entire ϕ and thus eventually solve (G1) is presented afterward.

Theorem 3: Let ϕ be the unique flow vector solving (G1), and ϕ' the flow vector minimizing (G2). Under Cond. 1–3, it holds $\phi'_\ell = \phi_\ell$ for all edges ℓ not belonging to active cycles.

Theorem 3 establishes that the only possible mismatches between ϕ' and ϕ occur only at the edges lying on cycles with compressors. Then, if there are no cycles with compressors, the GF problem is solved correctly; see also [8, Th. 2].

Corollary 1: Under Conditions 1 and 2, for an NGN without compressors in cycles, the minimizer of (G2) solves (G1) as well.

Corollary 1 identifies a setup where (G2) is equivalent to solving (G1). Nonetheless, if there are no compressors in cycles, one would prefer tackling (G1) using the solvers of Section IV. This is because running the decomposition technique discussed in Remark 1 and solving (7) are simpler than solving the MI-QCQP of (G2).

C. Recovering the GF Solution

Returning to the general setup, we next provide a procedure to retrieve the solution ϕ of (G1) given a minimizer ϕ' of (G2). From Theorem 3, vector ϕ' needs to be corrected only at the entries corresponding to edges in active cycles. To this end, we first put forth an algorithm to correct the flows within a single active cycle, and then delineate the steps to systematically correct the flows for all active cycles of the network.

Consider an active cycle $\mathcal{C}$ with $N_\mathcal{C}$ nodes. Let ψ_0 be a known pressure on node $0 \in \mathcal{C}$, and $\phi'_\mathcal{C}$ be the $N_\mathcal{C}$-length subvector of ϕ' collecting the flows on $\mathcal{C}$. Similarly, let $\mathbf{n}_\mathcal{C}$ be the $N_\mathcal{C}$-length subvector of the indicator vector for cycle $\mathcal{C}$. The following lemma explains how $\phi_\mathcal{C}$ can be recovered from $\phi'_\mathcal{C}$.

Lemma 4: Given a known pressure ψ_0, and flows $\phi'_\mathcal{C}$ on active cycle $\mathcal{C}$ obtained from (G2), Algorithm 1 determines the corrected GFs $\phi_\mathcal{C}$ such that the relaxed Weymouth equations in (11) are satisfied with equality.

Proof: Because ϕ and ϕ' both satisfy (2), it follows that $(\phi - \phi') \in \mathrm{null}(\mathbf{A}^\top)$. Since there are no overlapping cycles,

we have that $\phi_\mathcal{C} = \phi'_\mathcal{C} + \lambda_\mathcal{C} \mathbf{n}_\mathcal{C}$ for some $\lambda_\mathcal{C} \in \mathbb{R}$. To recover $\phi_\mathcal{C}$, we next provide a method for finding $\lambda_\mathcal{C}$.

Suppose one is given a $\lambda \in \mathbb{R}$. Given pressure ψ_0 and the candidate flow vector $\phi'_\mathcal{C} + \lambda \mathbf{n}_\mathcal{C}$, one can calculate the pressures along $\mathcal{C}$ sequentially using (3a) and (4a). Upon completing the cycle, the pressure at node $0 \in \mathcal{C}$ will be evaluated to the value of $\hat{\psi}_0(\lambda)$. The value $\hat{\psi}_0(\lambda)$ may not be equal to ψ_0. Note that for $\lambda > \lambda_\mathcal{C}$, it holds that

$$\mathrm{sign}(\phi'_\mathcal{C} - \phi_\mathcal{C} + \lambda \mathbf{n}_\mathcal{C}) \odot \mathbf{n}_\mathcal{C} = \mathrm{sign}((\lambda - \lambda_\mathcal{C}) \mathbf{n}_\mathcal{C}) \odot \mathbf{n}_\mathcal{C} > \mathbf{0}.$$

Using the above along with the argument used in the proof of Lemma 2, it can be shown that $\hat{\psi}_0(\lambda) < \psi_0$. In a similar fashion, if $\lambda < \lambda_\mathcal{C}$, then $\hat{\psi}_0(\lambda) > \psi_0$. Therefore, the function $\hat{\psi}_0(\lambda) - \psi_0$ is monotonic in λ, and $\hat{\psi}_0(\lambda) = \psi_0$ if and only if $\lambda = \lambda_\mathcal{C}$. Thanks to this monotonicity, one can find $\lambda_\mathcal{C}$ iteratively using bisection, tabulated as Algorithm 1.

Lemma 4 shows that $\phi_\mathcal{C}$ can be recovered from ψ_0 and $\phi'_\mathcal{C}$ using a bisection technique on λ. The limits for the search space $[\underline{\lambda}, \overline{\lambda}]$ of λ can be found using engineering constraints on GFs. In fact, these limits can be tightened since the entries of $\phi'_\mathcal{C}$ and $\phi_\mathcal{C}(\lambda) = \phi'_\mathcal{C} + \lambda \mathbf{n}_\mathcal{C}$ corresponding to any compressor in $\mathcal{C}$ must have the same sign due to (4b).

We next provide the steps to find the correct GF solution using the flow ϕ' obtained from (G2).

T1) Select a spanning tree $\mathcal{T}$ of the NGN graph $\mathcal{G}$ rooted at the reference node r.

T2) Starting from node r, traverse $\mathcal{T}$ via a depth-first search.

T3) If a node n does not belong to an active cycle of $\mathcal{G}$, calculate its pressure as follows: If the edge connecting node n to its parent node in $\mathcal{T}$ is a lossy pipe, use (3a); else, if this edge is a compressor, use (4a).

T4) If a node n belongs to an active cycle $\mathcal{C}$, check if the flows in cycle $\mathcal{C}$ have been corrected. If the flows are already corrected or if i is the first node in $\mathcal{C}$ that is encountered, compute the nodal pressure as in step *T3)*. Else, pass the pressure at the parent node of i (which is also in $\mathcal{C}$) along with the noncorrected flow subvector $\phi'_\mathcal{C}$ to Algorithm 1 and obtain the corrected flows on $\mathcal{C}$.

T5) Continue until all nodes in $\mathcal{T}$ have been traversed.

VI. COMPARISON TO PRIOR WORK

This article puts forth three novel components: *c1)* proving the uniqueness of the GF problem solution under steady-state conditions; *c2)* proposing GF solvers based on the energy function minimization; and *c3)* devising a provably exact MI-QCQP relaxation. These components are next contrasted to existing related works:

c1) Uniqueness: For an NGN with no compressors, the GF solution may be found as a minimizer of (7); see [12] and [23]. A linearization technique has also been put forth to accelerate solving (7) [23]. Papers [9] and [13] broaden the uniqueness claim for NGNs with *additive* compressors of constant gain. These works formulate strictly convex problems that yield a GF solution; hence proving uniqueness by convexity. However, gas compressors are oftentimes *multiplicative*, so that the previous uniqueness claims do not carry over. In our work [8], uniqueness was proved for multiplicative compressors under any network

Algorithm 1: Recover Flows on Active Cycles Upon Solving (G2).

Input	: $\psi_0, \phi'_{\mathcal{C}}, \mathbf{n}_{\mathcal{C}}, \underline{\lambda}, \overline{\lambda}$; tolerance ϵ; pipe and compressor parameters along $\mathcal{C}$
Output	: flow vector $\phi_{\mathcal{C}}$ and pressure vector $\psi_{\mathcal{C}}$ along $\mathcal{C}$

Initialize: Set $\lambda \leftarrow \frac{\underline{\lambda}+\overline{\lambda}}{2}$ and $\psi_0(\lambda) \leftarrow \infty$

while $|\psi_0(\lambda) - \psi_0| \geq \epsilon$ **do**

  Try flow vector $\phi'_{\mathcal{C}} + \lambda \mathbf{n}_{\mathcal{C}}$. Starting from node 0, compute pressures $\psi_n(\lambda)$ along all nodes in $n \in \mathcal{C}$ using (3a) and (4a) until you return to node 0.

  if $\psi_0(\lambda) > \psi_0$ **then**

    | Set $\underline{\lambda} \leftarrow \lambda, \ \lambda \leftarrow \frac{\underline{\lambda}+\overline{\lambda}}{2}$

  else

    | Set $\overline{\lambda} \leftarrow \lambda, \ \lambda \leftarrow \frac{\underline{\lambda}+\overline{\lambda}}{2}$

  end

end

Return : flows $\phi_{\mathcal{C}} = \phi'_{\mathcal{C}} + \lambda \mathbf{n}_{\mathcal{C}}$ and pressures $\psi_{\mathcal{C}}(\lambda)$

Fig. 1. *Top:* Modified Belgian NGN. *Bottom:* GasLib-40 network with red edges representing compressors.

topology, but with a single fixed-pressure node. Theorem 2 generalizes all past claims for NGNs with multiplicative compressors, any topology, and an arbitrary number of fixed-pressure nodes.

c2) Energy function minimization: Problem (7) dates back to [12], and has since been used for solving the GF task; verifying the feasibility and uniqueness of a GF instance [23]; and initializing optimization problems. However, its applicability was limited to NGNs without compressors. As explained in Remark 1, this work suggests using (7) to handle NGNs with compressors on nonoverlapping cycles. We also present the unconstrained energy function formulation of (8).

c3) MI-QCQP relaxation of GF: The key difficulty in solving (optimal) GF problems stems from the nonlinear Weymouth equation. A disjunctive convex relaxation of this equation was found to be efficient in [4] and [22]. Numerous studies have thereon employed similar convex relaxations; see [5], [7], and [26]. Unfortunately, it is hard to guarantee the exactness of these relaxations. An effective heuristic is to fix the binary variables involved to the values obtained by the convex relaxation and handle the resultant nonconvex nonlinear program through a general solver [4], [5]. A gas-electric flow problem was solved in [26], wherein a cost function was proposed that was numerically found useful toward attaining exact relaxation. Unlike previous works, the MI-QCQP formulation of Section V provides theoretical guarantees for exact relaxation, while expanding the claims of [8]. The GF solver developed in [8] was applicable to NGNs with compressors not on cycles. However, in this work, the cost function of (G2) is meticulously designed to ensure that correct flows are obtained outside active cycles. Additionally, Algorithm 1 is developed to enable flow correction on active cycles efficiently. Although the GF problem is intrinsically simpler than the optimal gas (and possible electric) flow problem considered in prior works, this article lays a foundation toward analytical guarantees for exact relaxation. It has been recently shown that exact relaxation of network flow optimization problems may be guaranteed using a convex penalty [27]. It is worth mentioning that a related MI-QCQP formulation of
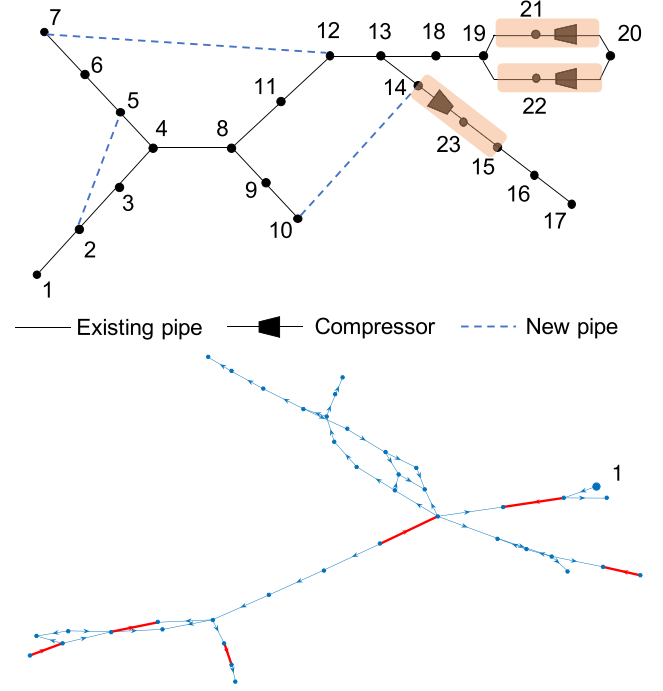
the water flow problem in [19], can also provably yield an *exact* convex relaxation for the optimal water flow task [20].

VII. NUMERICAL TESTS

The proposed GF solver based on the relaxed MI-QCQP (G2) and Algorithm 1 was tested on the modified Belgian benchmark NGN and the GasLib-40 NGN of Fig. 1. Starting with the Belgian NGN, the pipe coefficients and compressor ratios were derived based on the nodal pressures and edge flows reported in [12]. The network contains three compressors, which are modeled as ideal compressors followed by lossy pipes. Problem (G2) was solved using the MATLAB-based optimization toolbox YALMIP using CPLEX as the MI-QCQP solver [28], [29]. All tests were conducted on a 2.7-GHz Intel Core i5 computer with 8 GB RAM.

As a model validation step, we first tested the (G2) solver on the original Belgian network, which is a tree, except for one cycle formed by parallel compressors (see Fig. 1). The pressure at node 1 was treated as a reference. The flow values obtained from (G2) agreed with those of [12] for all edges except for the edges along the active cycle. Similarly, the pressures agreed for all nodes other than node 20. Therefore, the pressure at node 19 and the flows on edges (19, 21), (19, 22), (20, 21), (20, 22) were passed to Algorithm 1 for correction. The final result was found to coincide with [12].

The Belgian network was subsequently augmented by additional pipelines (see Fig. 1). The resulting modified network has overlapping cycles, thus violating Condition 2 required in Theorem 3. To get reasonable friction coefficients, for every added line (m, n), the coefficient a_{mn} was set equal to the
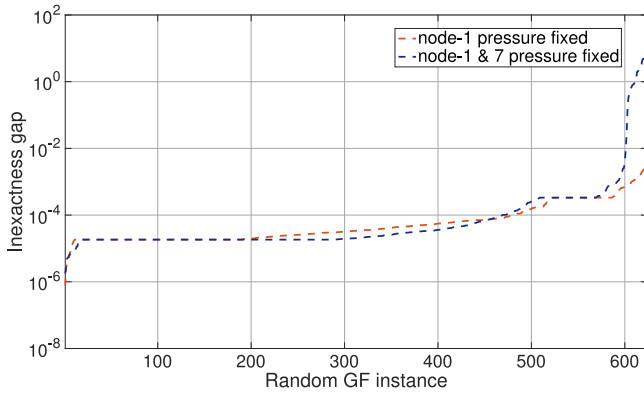
Fig. 2.   Inexactness gap attained by (G2) followed by Algorithm 1 over random feasible instances of the GF problem.

Fig. 3.   Running time for (G2) and Algorithm 1 over random feasible GF instances.

sum of $a'_\ell s$ along the $m - n$ path, yielding $a_{2,5} = 0.1936$, $a_{10,14} = 0.0439$, $a_{7,12} = 0.0419$. We kept the reference pressure at node 1 and the compression ratios constant as in [12], and drew 1500 random gas injections $\mathbf{q}$. To construct these samples, we perturbed the benchmark injections $\mathbf{q}_0$ that lie in the range $[-15.61, 22.01]$ by a standardized normal deviation. The injection at node 20 was set to the negative sum of the remaining injections to get $\mathbf{1}^\top \mathbf{q} = 0$ for all samples.

Using the modified meshed Belgian NGN of Fig. 1 and the random gas injections, we tested the exactness of (G2) and the performance of Algorithm 1. Not all of the random injections were feasible for the GF problem – some violated (4b) or (3b). Problem (G2) was infeasible for 876 out of the 1,500 random instances. Since (G2) is a relaxation of (G1), these instances are apparently infeasible for (G1) too. The performance of (G2) and Algorithm 1 was tested on the remaining 624 gas injection instances. To evaluate the success of (G2) in solving (G1), we calculated the *inexactness gap* G defined as

$$G := \max_{(m,n) \in \bar{\mathcal{P}}_a} \frac{|\psi_m - \psi_n| - a_{mn}\phi_{mn}^2}{a_{mn}\phi_{mn}^2} \geq 0$$

for the pressures and flows obtained by (G2) and Algorithm 1.

The ranked inexactness gap for the feasible GF instances is shown by the first curve in Fig. 2. The gap was less than 10^{-3} for more than 97% of the feasible instances, while the maximum gap over all instances was 0.009. This corroborates that the proposed solver performs well even when Condition 2 is not met. Fig. 3 shows the running time for solving (G2) and Algorithm 1 over the 624 feasible instances. The average (median) running time was 0.96 s (0.89 s).

Considering Condition 1, we used the fixed pressure at node 1 and the pressures obtained at node 7 for the feasible GF instances, we solved (G2) again. Although the hypothesis of Theorem 3 does not hold anymore, the inexactness gap was found to be less than 10^{-3} for more than 94% of the instances; see the second curve in Fig. 2. Thus, the tests reveal that the novel solver successfully finds the GF solution even when the sufficient Conditions 1 and 2 are violated. However, Condition 3 prohibiting gas circulations could not be violated for the Belgian NGN because the only active cycle in this NGN has parallel compressors, hence avoiding circulations from (4b). We next
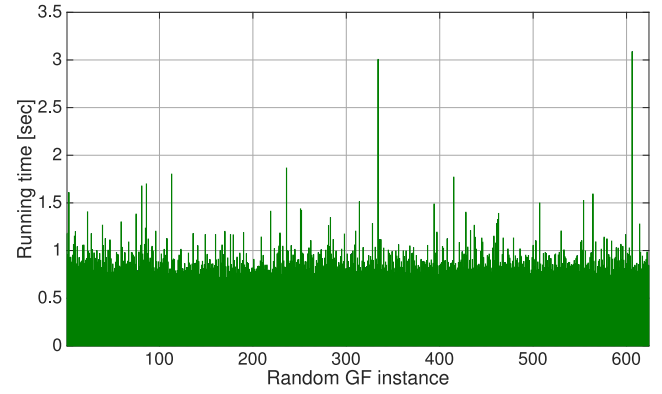
deal with GF instances on the GasLib-40 network, wherein a circulation could potentially occur.

GasLib-40 roughly represents a part of the German gas transport network [30]. The network exhibits 40 nodes, 39 pipes, and 6 compressors [see Fig. 1 (*bottom*)]. The pipe dimensions, roughness coefficients, and a nominal demand vector $\mathbf{q}_0$ were derived from [30]. The goals for conducting additional tests on GasLib-40 include the following conditions:

1) evaluating our solvers on a realistic setup;
2) testing our MI-QCQP when Condition 3 is violated;
3) benchmarking the performance of our solvers against the NR-based solver.

We next briefly introduce the NR-based solver used for benchmarking. Given an injection $\mathbf{q}$, compressor ratios $\alpha_\ell s$ and reference pressure ψ_1 stack the unknowns as $\mathbf{y} = [\phi_1, \ldots, \phi_L, \psi_2, \ldots, \psi_N]^\top$. Define the equality constraints (2), (3a), and (4a) collectively as $\mathbf{g}(\mathbf{y}) = \mathbf{0}$. Given an initial estimate $\mathbf{y}_0$, the NR-based solver would iterate as

$$\mathbf{y}_{t+1} = \mathbf{y}_t - \mu[\mathbf{J}(\mathbf{y}_t)]^{-1}\mathbf{g}(\mathbf{y}_t)$$

where t is the iteration count, matrix $\mathbf{J}(\mathbf{y}_t)$ is the Jacobian of $\mathbf{g}(\mathbf{y})$ evaluated at $\mathbf{y}_t$, and μ a step size. A solution $\mathbf{y}^\star$ obtained on the convergence of NR updates would be deemed feasible if the inequalities (3b) and (4b) are satisfied. Since the NR updates target at attaining $\mathbf{g}(\mathbf{y}) = \mathbf{0}$, the performance evaluation criteria for our results would be $\|\mathbf{g}(\mathbf{y})\|_2$ in lieu of the inexactness gap G.

In the first set of tests on GasLib-40, we generated 500 gas injection instances $\mathbf{q}$ by scaling the entries of $\mathbf{q}_0$ independently, by random factors chosen uniformly on [0.75,1.25]. The pressure at node 1 was set to 50 bar and its injection was set to the negative sum of other nodes for all instances. Next, the compression ratios for the six compressors were drawn uniformly within [1, 2]. All 500 instances were solved using three approaches: *a1*) the MI-QCQP and Algorithm 1; *a2*) NR with flows initialized at $(\mathbf{A}^\top)^\dagger\mathbf{q}$, and all pressures initialized at ψ_1; and *a3*) NR with flows and pressures initialized at the solution of MI-QCQP and Algorithm 1. The stopping criteria for NR were set to $\|\mathbf{g}(\mathbf{y})\|_2 < 10^{-3}$, subject to a maximum iteration count of 50. The step size for both initialization scenarios was kept as $\mu = 1$. The MI-QCQP deemed five out of the 500 instances
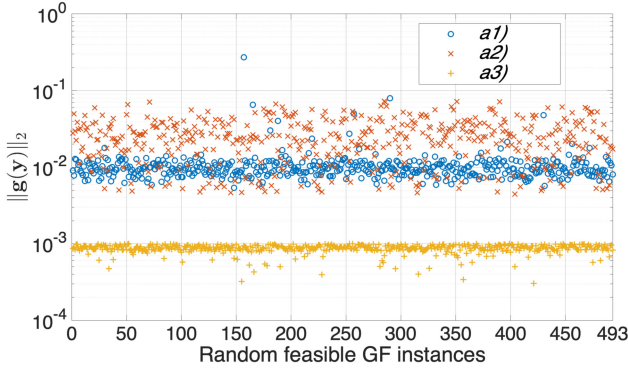
Fig. 4. Accuracy measure $\|\mathbf{g}(\mathbf{y})\|_2$ for GF solutions obtained by MI-QCQP in (G2) followed by Algorithm 1, and GF solutions found by the NR iterations for different initializations.

as infeasible and the performance criteria $\|\mathbf{g}(\mathbf{y})\|_2$ was found to lie in $[0.005, 0.183]$ with the median at 0.009. To compare to the index of the inexactness gap, the range for G for the 495 feasible cases was $[8 \cdot 10^{-5}, 6 \cdot 10^{-2}]$. Thus, the MI-QCQP alongside Algorithm 1 was successful in finding the GF solution for all 495 instances. Interestingly, 474 of the 495 feasible GF instances exhibit circulations, and hence violate Condition 3. Thus, the numerical results empirically demonstrate that the developed MI-QCQP alongside Algorithm 1 successfully solves the GF problem even when the conditions of Theorem 3 are violated. The NR solver, if initialized at the solution of MI-QCQP improves the solution accuracy, resulting in $\|\mathbf{g}(\mathbf{y}^\star)\|_2$ within $1.2 \cdot 10^{-4} - 0.13$. For the five instances deemed infeasible by MI-QCQP, the NR solver was initialized at all zero flows and pressures; all five instances failed to converge. Surprisingly, when the NR solver was initialized with $(\mathbf{A}^\top)^\dagger \mathbf{q}$ as flows and $\psi_0' s$ as pressures, all 500 instances failed to converge. The nonconvergence of the NR solver is however alleviated when μ was reduced as discussed next.

A second set of tests were conducted on the GasLib-40 NGN with 500 random injections and compressor ratios generated as described earlier. The MI-QCQP solver deemed seven of the 500 instances as infeasible. All 500 instances were then solved with the NR-based solver with flows initialized at $(\mathbf{A}^\top)^\dagger \mathbf{q}$ and pressures at ψ_1, and μ was set to $\mu = 0.9$. A steep decline in $\|\mathbf{g}(\mathbf{y}_t)\|_2$ was observed in the first few (roughly 10) iterations, while the tolerance of 10^{-3} was not attained within the 50 iterations limit. However, if the NR solver is initialized at the solution of MI-QCQP and Algorithm 1, the convergence criteria of 10^{-3} were attained at an average of 7.8 iterations. The values of $\|\mathbf{g}(\mathbf{y})\|_2$ attained by three solution techniques *a1)*–*a3)* are shown in Fig. 4. The results suggest that the accuracy of the MI-QCQP solver is better than that of *a2)*, which is a prudent initialization. However, if the NR-based solver is warm-started with the solution of MI-QCQP, an order of magnitude improvement in accuracy is observed. On the computational front, the MI-QCQP solver alongside Algorithm 1 is efficient with the median solving time of 1.52 s. However, as anticipated, the NR solvers have superior performance with median solving time of 0.17 s. Finally, inspecting the seven instances deemed infeasible by the MI-QCQP solver, the solution obtained by *a2)* indicates
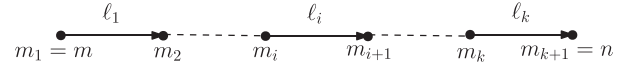

Fig. 5. Nomenclature for nodes and edges along $\mathcal{P}_{mn}$.

violation of (4b), demonstrating the merit of the proposed MI-QCQP toward certifying infeasibility of GF instances.

VIII. CONCLUSION

Exploiting recent results from graph theory and convex relaxations, this article provides a fresh perspective on the steady-state GF problem. The uniqueness of the GF solution has been established in a generalized setting for arbitrary NGN topologies, multiplicative compressors and multiple fixed-pressure nodes. Granted that the GF solution is unique, constrained and unconstrained versions of convex energy function minimization-based GF solvers have been proposed. These solvers can efficiently solve any GF task instance with a single fixed-pressure node and networks with compressors not on cycles. To expand the scope, an MI-QCQP GF solver had been also proposed relying on a convex relaxation of the Weymouth equation. The relaxation has been shown to be exact under specific network conditions. Numerical tests reveal that the developed MI-QCQP solver succeeds in finding the unique GF solution even when the needed conditions are violated. The success of the MI-QCQP relaxation is attributed to a judiciously designed objective. The developed approach sets forth an analytical platform for ensuring exact relaxation. Evaluating the performance of the developed approach for various optimal GF tasks constitutes an interesting research direction.

APPENDIX

Proof of Lemma 2: For an edge $\ell_i \in \mathcal{P}_{mn}$, let us name the incident node closer to m as m_i, and the other node as m_{i+1}, as shown in Fig. 5.

Let $\boldsymbol{\psi}$ and $\boldsymbol{\psi}'$ be the pressure vectors corresponding to $\boldsymbol{\phi}$ and $\boldsymbol{\phi}'$. Since pressures ψ_m and ψ_n are fixed, it follows $\psi_m = \psi'_m$ and $\psi_n = \psi'_n$. Proving by contradiction, suppose (5a) holds. If that is the case, first it will be shown that $\psi'_{m_i} - \psi'_{m_{i+1}} > \psi_{m_i} - \psi_{m_{i+1}}$ for every lossy pipe $\ell_i \in \mathcal{P}_{mn}$.

Suppose that $\operatorname{sign}(\boldsymbol{\phi}' - \boldsymbol{\phi}) \cdot \boldsymbol{\pi}^{mn} > 0$. Let us denote the right-hand side (RHS) of (3a) by $w(\phi_\ell)$. It is evident that $w(\phi_\ell)$ is monotonically increasing in ϕ_ℓ. Hence, for any lossy pipe $\ell_i \in \mathcal{P}_{mn}$, it holds

$$
\begin{aligned}
0 &\stackrel{a}{<} \pi_{\ell_i}^{mn} \operatorname{sign}(\phi'_{\ell_i} - \phi_{\ell_i}) \\
&\stackrel{b}{=} \pi_{\ell_i}^{mn} \operatorname{sign}(w(\phi'_{\ell_i}) - w(\phi_{\ell_i})) \\
&\stackrel{c}{=} \operatorname{sign}(\pi_{\ell_i}^{mn}) \operatorname{sign}(w(\phi'_{\ell_i}) - w(\phi_{\ell_i})) \\
&\stackrel{d}{=} \operatorname{sign}(\pi_{\ell_i}^{mn} w(\phi'_{\ell_i}) - \pi_{\ell_i}^{mn} w(\phi_{\ell_i})) \\
&\stackrel{e}{=} \operatorname{sign}((\psi'_{m_i} - \psi'_{m_{i+1}}) - (\psi_{m_i} - \psi_{m_{i+1}}))
\end{aligned}
\tag{12}
$$

where (a) holds by hypothesis, (b) stems from the monotonicity of $w(\phi_\ell)$, (c) holds because $\pi_{\ell_i}^{mn} \in \{0, 1, -1\}$, (d) holds from the property of sign by definition, and (e) from the definition of

Fig. 6.   Augmented NGN graph.

Fig. 7.   Four possible scenarios for a cycle with noncirculating GF. The arrows represent the actual GF directions.

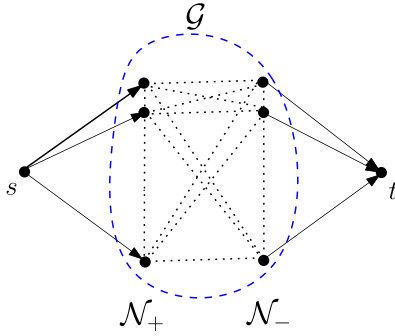π^{mn} and (3a). The inequality (12) implies

$$\psi'_{m_i} - \psi'_{m_{i+1}} > \psi_{m_i} - \psi_{m_{i+1}}. \qquad (13)$$

Let us now apply (13) and (4a) for the edges ℓ_1 to ℓ_k along $\mathcal{P}_{mn}$. For the fixed-pressure node m, we have $\psi_m = \psi'_m$. If ℓ_1 is a lossy pipe, we get $\psi'_{m_2} < \psi_{m_2}$ from (13); otherwise $\psi'_{m_2} = \psi_{m_2}$ from (4a). Similarly, we can show that $\psi'_{m_3} \leq \psi_{m_3}$, where the equality holds only if both ℓ_1 and ℓ_2 are compressors. However, this is practically impossible as every compressor is modeled as an ideal compressor followed by a lossy pipe, necessitating $\psi'_{m_3} < \psi_{m_3}$. Continuing the process for all edges along $\mathcal{P}_{mn}$ yields $\psi'_n < \psi_n$, which contradicts with node n being a fixed-pressure node. Similarly, the assumption $\text{sign}(\phi' - \phi) \cdot \pi^{mn} < 0$ leads to a contradiction by yielding $\psi'_n > \psi_n$. ∎

Proof of Lemma 3: Given the two pairs $(\mathbf{q}, \phi)$ and $(\mathbf{q},' \phi')$ satisfying (2) and $\mathbf{q} \neq \mathbf{q}'$, let us define $\tilde{\phi} := \phi' - \phi$ and $\tilde{\mathbf{q}} := \mathbf{q}' - \mathbf{q}$. By applying (2) on $(\mathbf{q}, \phi)$ and $(\mathbf{q},' \phi')$, and taking the difference, we get

$$\mathbf{A}^\top \tilde{\phi} = \tilde{\mathbf{q}}. \qquad (14)$$

Since $\mathbf{1} \in \text{null}(\mathbf{A})$, premultiplying (14) by $\mathbf{1}^\top$ provides

$$\mathbf{1}^\top \tilde{\mathbf{q}} = \mathbf{0}. \qquad (15)$$

From (14) and (15), the pair $(\tilde{\mathbf{q}}, \tilde{\phi})$ qualifies as a set of balanced gas injections. By definition of $(\tilde{\mathbf{q}}, \tilde{\phi})$, proving (6) is equivalent to showing there exists a path $\mathcal{P}_{mn}$ for which

$$\tilde{\phi} \odot \pi^{mn} > \mathbf{0} \qquad (16a)$$

$$\tilde{q}_m > 0 \text{ and } \tilde{q}_n < 0. \qquad (16b)$$

To prove the existence of such a path, we use the ensuing result based on [31, Th. 8.8]. ∎

Lemma 5 (see [31]): Given a graph with injection q at node s, demand q at node t, and zero injections at all other nodes, there exists an s–t path with flow directions along the path from s to t:

Lemma 5 considers a single-source single-destination network flow setup. We transform our problem to this setup through the following steps (see also Fig. 6):

1) The nodes of graph $\mathcal{G}$ are partitioned into the subset with positive $\mathcal{N}_+ : \{n \in \mathcal{N} : \tilde{q}_n > 0\}$; negative $\mathcal{N}_- : \{n \in$
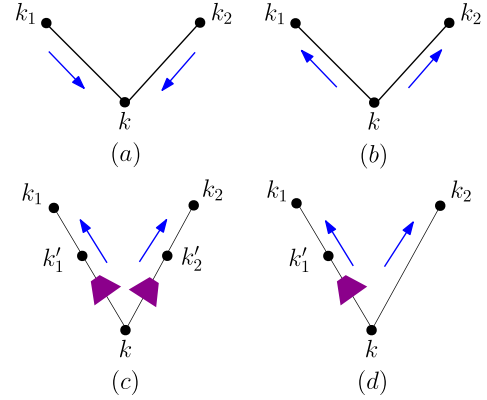
$\mathcal{N} : \tilde{q}_n < 0\}$; and zero injections $\mathcal{N}_0 : \{n \in \mathcal{N} : \tilde{q}_n = 0\}$. Because $\tilde{\mathbf{q}} \neq \mathbf{0}$, the sets $\mathcal{N}_+$ and $\mathcal{N}_-$ are nonempty.
2) Augment $\mathcal{G}$ by adding nodes s and t.
3) All nodes in $\mathcal{N}_+$ are connected to node s, and all nodes in $\mathcal{N}_-$ are connected to node t.
4) The injections in $\mathcal{N}_+$ are lumped in node s by setting the flows $\tilde{\phi}_{sn} = \tilde{q}_n$ for all $n \in \mathcal{N}_+$. Similarly, the demands in $\mathcal{N}_-$ are lumped in node t by setting the flows $\tilde{\phi}_{nt} = -\tilde{q}_n$ for all $n \in \mathcal{N}_-$.

Applying Lemma 5 on this augmented graph, there exists a path $\mathcal{P}_{st}$ with flow directions from s to t. For any such path $\mathcal{P}_{st}$, eliminate the first and last edges to get a path $\mathcal{P}_{mn}$ with $m \in \mathcal{N}_+$ and $n \in \mathcal{N}_-$. Claim (16b) follows by construction. We next show (16a): For each edge $\ell \in \mathcal{P}_{mn}$, it was shown that the direction of $\tilde{\phi}_\ell$ is along the path $\mathcal{P}_{mn}$. If $\pi_\ell^{mn} = +1$, the direction of edge ℓ agrees with the direction of $\mathcal{P}_{mn}$. Since $\tilde{\phi}_\ell$ is along $\mathcal{P}_{mn}$, then $\tilde{\phi}_\ell > 0$. If $\pi_\ell^{mn} = -1$, the direction of edge ℓ is opposite to the direction of $\mathcal{P}_{mn}$. Since $\tilde{\phi}_\ell$ is along $\mathcal{P}_{mn}$, then $\tilde{\phi}_\ell < 0$. Either way, it holds that $\tilde{\phi}_\ell \pi_\ell^{mn} > 0$ for all $\ell \in \mathcal{P}_{mn}$, which proves (6a).

Proof of Theorem 3: Before proving the main result, we will need two preliminary results. ∎

Lemma 6: For a lossy pipe $\ell = (m, n)$ not on an active cycle, if the triplet $(\psi_m, \psi_n, \phi_\ell)$ satisfies (11), then the triplet $(\psi_m + \delta, \psi_n + \delta, \phi_\ell)$ also satisfies (11) for any finite δ.

Lemma 6 follows directly from the fact that (11) involves pressure differences rather than pressures.

Lemma 7: Consider an active cycle $\mathcal{C}_0$ and index its nodes as $\{0, \dots, k\}$. Given a fixed pressure ψ_0 and flows $\{\phi_\ell\}_{\ell \in \mathcal{C}_0}$ satisfying Condition 3 and (4b), there exists a set of pressures $\{\psi_i\}_{i=1}^k$ satisfying (11) and (4a).

Proof: From Condition 3 and the fact that a compressor is modeled as an ideal compressor followed by a lossy pipe, it is not hard to see that there must exist a node $k \in \mathcal{C}_0$ that leads to one of the four flow scenarios shown in Fig. 7.

Proving by construction, we will next define pressures $\{\psi_i\}_{i=1}^k$ such that (11) and (4a) are satisfied for all edges in $\mathcal{C}_0$. Traversing the paths $0 \to k_1$ and $0 \to k_2$, one can recursively define pressures for all nodes using ψ_0 and flows $\{\phi_\ell\}_{\ell \in \mathcal{C}_0}$ based on the exact Weymouth equation (3) and (4a). The pressures on

the remaining nodes of $\mathcal{C}_0$ can be defined for the four scenarios of Fig. 7 as follows:

$$(a)\psi_k := \min\{\psi_{k_1} - a_{k_1 k}\phi_{k_1 k}^2, \psi_{k_2} - a_{k_2 k}\phi_{k_2 k}^2\}$$

$$(b)\psi_k := \max\{\psi_{k_1} + a_{kk_1}\phi_{kk_1}^2, \psi_{k_2} + a_{kk_2}\phi_{kk_2}^2\}$$

$$(c)\psi_k := \max\left\{\frac{\psi_{k_1} + a_{k_1' k_1}\phi_{k_1' k_1}^2}{\alpha_{kk_1'}}, \frac{\psi_{k_2} + a_{k_2' k_2}\phi_{k_2' k_2}^2}{\alpha_{kk_2'}}\right\}$$

$$\psi_{k_1'} := \alpha_{kk_1'}\psi_k, \quad \psi_{k_2'} := \alpha_{kk_2'}\psi_k$$

$$(d)\psi_k := \max\left\{\frac{\psi_{k_1} + a_{k_1' k_1}\phi_{k_1' k_1}^2}{\alpha_{kk_1'}}, \psi_{k_2} + a_{kk_2}\phi_{kk_2}^2\right\}$$

$$\psi_{k_1'} := \alpha_{kk_1'}\psi_k.$$

To see that the constructed pressures satisfy (11), take, for example, scenario (a). Applying (11) along the edges (k_1, k) and (k_2, k) yield that ψ_k should satisfy $\psi_k \leq \psi_{k_1} - a_{k_1 k}\phi_{k_1 k}^2$ and $\psi_k \leq \psi_{k_2} - a_{k_2 k}\phi_{k_2 k}^2$. This is indeed the case by selecting ψ_k as the minimum of the two RHS. Similar reasoning applies to the other scenarios. ∎

Proceeding with the proof of Theorem 3, let (ϕ, ψ) be the unique solution to (G1), and $(\phi,' \psi')$ a minimizer of (G2). Proving by contradiction, assume that there exists an edge ℓ not belonging to an active cycle, such that $\phi_\ell' \neq \phi_\ell$. Recall that the set of all active cycles is denoted by $\mathcal{S}_\mathcal{C}^a$. Since both flow vectors satisfy (2), their difference $\mathbf{n} := \phi - \phi'$ must lie in the nullspace of $\mathbf{A}^\top$. The nullspace of $\mathbf{A}^\top$ is spanned by the indicator vectors for all fundamental cycles in the gas network graph [32, Corollary 14.2.3]. Therefore, the entries of $\mathbf{n}$ related to edges not on a cycle must be zero. Since by hypothesis $\ell \notin \mathcal{S}_\mathcal{C}^a$, edge ℓ should belong to one of the cycles in $\mathcal{S}_\mathcal{C} \setminus \mathcal{S}_\mathcal{C}^a$. This nonactive cycle will be henceforth termed $\mathcal{C}$.

The rest of the proof is organized in three parts: Part I constructs a flow vector $\hat{\phi}$ that satisfies (2) and (4b). Part II shows there exists a $\hat{\psi}$ so that the pair $(\hat{\phi}, \hat{\psi})$ is feasible for (G2). Part III shows that $(\hat{\phi}, \hat{\psi})$ attains a smaller objective for (G2), thus contradicting the optimality of $(\phi,' \psi')$.

Part I: Define the flow vector $\hat{\phi}$ as

$$\hat{\phi}_\ell := \begin{cases} \phi_\ell, & \ell \in \mathcal{C} \\ \phi_\ell, & \ell \text{ belongs to any active cycle} \\ \phi_\ell,' & \text{otherwise.} \end{cases} \quad (17)$$

By construction, vector $\hat{\phi}$ satisfies

$$\phi' - \hat{\phi} = \lambda\mathbf{n}^\mathcal{C} + \mathbf{n}^a \quad (18)$$

where $\mathbf{n}^\mathcal{C}$ is the indicator vector for cycle $\mathcal{C}$, the constant λ is nonzero, and vector $\mathbf{n}^a \in \text{null}(\mathbf{A}^\top)$ can have nonzero entries only for edges in active cycles. Since ϕ' satisfies constraint (2) and $\mathbf{A}^\top\mathbf{n}^\mathcal{C} = \mathbf{A}^\top\mathbf{n}^a = \mathbf{0}$, then $\mathbf{A}^\top\hat{\phi} = \mathbf{A}^\top\phi' = \mathbf{q}$. This proves that $\hat{\phi}$ satisfies (2). Note that $\hat{\phi}$ is constructed by selecting entries from ϕ and ϕ'. Granted both ϕ and ϕ' satisfy (4b), vector $\hat{\phi}$ trivially satisfies (4b) too.

Part II: We will delineate the steps for constructing a vector of pressures $\hat{\psi}$ such that $(\hat{\phi}, \hat{\psi})$ is feasible for (G2). Let us select a spanning tree $\mathcal{T}$ of the NGN graph $\mathcal{G}$ rooted at the reference r. We shall define the pressures $\hat{\psi}_n$s while traversing $\mathcal{T}$ via depth-first search. In such a traversal, the following three cases may be identified on arriving at any node n.

Case 1: Node n is neither in $\mathcal{C}$ nor on an active cycle. Let $n-1$ be the parent node of n in $\mathcal{T}$ and define

$$\hat{\psi}_n := \begin{cases} \alpha_{n-1,n}\hat{\psi}_{n-1}, & \text{if } (n-1, n) \in \mathcal{P}_a \\ \hat{\psi}_{n-1} + (\psi_n' - \psi_{n-1}'), & \text{if } (n-1, n) \in \bar{\mathcal{P}}_a. \end{cases}$$

Since the edge $(n-1, n)$ is not in $\mathcal{C} \cup \mathcal{S}_\mathcal{C}^a$, we have $\hat{\phi}_{n-1,n} = \phi_{n-1,n}'$ from (17). Therefore, if $(n-1, n)$ is a lossy pipe, Lemma 6 ensures that the defined pressure $\hat{\psi}_n$ satisfies (11). Moreover, if $(n-1, n)$ is a compressor, constraint (4a) is satisfied trivially by definition.

Case 2: Node n is in $\mathcal{C}$. If n is the first node in $\mathcal{C}$ to be visited, define $\hat{\psi}_n$ as in *Case 1*. Then, define the pressures for the remaining nodes $i \in \mathcal{C}$ as $\hat{\psi}_i := \psi_i + (\hat{\psi}_n - \psi_n)$. Note from (17) that the flows along $\mathcal{C}$ are assigned from ϕ, the pair (ϕ, ψ) satisfies (3) and hence the relaxed Weymouth (11) as well. The constructed pressures $\hat{\psi}_i$s for $i \in \mathcal{C}$ are simply a shifted version of the pressures ψ_is. Therefore, the pressures $\hat{\psi}_i$s satisfy (11) from Lemma 6. Mark all nodes in $\mathcal{C}$ as traversed and continue.

Case 3: Node n is in an active cycle $\mathcal{C}_a$. If n is the first node in $\mathcal{C}_a$ to be traversed, define the $\hat{\psi}_n$ as in *Case 1*. Then, define the pressure for the remaining nodes $i \in \mathcal{C}_a$ using Lemma 7. Mark all nodes in $\mathcal{C}_a$ as traversed and continue.

Since the constructed pressures satisfy (11) and (4a), the pair $(\hat{\phi}, \hat{\psi})$ is feasible for (G2). Observe that the pressure drop across lossy pipes not in $\mathcal{C}$ is $\hat{\psi}_m - \hat{\psi}_n = \psi_m' - \psi_n'$ for *Case 1*; and $\hat{\psi}_m - \hat{\psi}_n = \psi_m - \psi_n$ for lossy pipes in $\mathcal{C}$ under *Case 2*. This fact is imperative for the ensuing Part III.

Part III: We will next show that $r(\psi') > r(\hat{\psi})$ to contradict the optimality of ψ'. Note that the objective $r(\psi)$ in (G2) sums up the absolute pressure differences along lossy pipes, but not on active cycles. Since by construction these differences have changed only along $\mathcal{C}$, we get

$$r(\psi') - r(\hat{\psi}) = \sum_{(m,n)\in\mathcal{C}} |\psi_m' - \psi_n'| - |\hat{\psi}_m - \hat{\psi}_n|. \quad (19)$$

As the pressure differences depend on flows, we next compare the entries of $\hat{\phi}$ and ϕ' along $\mathcal{C}$ using (18). Since the edge directions are assigned arbitrarily, assume wlog that $\hat{\phi}_{mn} \geq 0$ for all $(m, n) \in \mathcal{C}$. Given $\mathbf{n}_\mathcal{C}$ and (18), one can find the value of λ. If $\lambda < 0$, reverse the reference direction for cycle $\mathcal{C}$ to get a positive λ. Because of this, we can assume $\lambda > 0$.

Recall that $\mathbf{n}_\mathcal{C} \in \{0, \pm 1\}^P$. Partition the set of edges in $\mathcal{C}$ into mutually exclusive sets $\hat{\mathcal{P}}_+$ and $\hat{\mathcal{P}}_-$ based on positive and negative entries of $\mathbf{n}_\mathcal{C}$, respectively. From (18), it follows

$$0 \leq \hat{\phi}_\ell < \phi_\ell' \quad \forall\ell \in \hat{\mathcal{P}}_+. \quad (20)$$

Summing up the pressure drops along $\mathcal{C}$ for $\hat{\psi}$ should be zero. Since the pressure drops along $\mathcal{C}$ are positive for the edges in $\hat{\mathcal{P}}_+$, and negative along the edges in $\hat{\mathcal{P}}_-$, it holds that

$$\sum_{(m,n)\in\hat{\mathcal{P}}_+} (\hat{\psi}_m - \hat{\psi}_n) = \sum_{(m,n)\in\hat{\mathcal{P}}_-} (\hat{\psi}_m - \hat{\psi}_n)$$

$$\Rightarrow \sum_{(m,n)\in\mathcal{C}} |\hat{\psi}_m - \hat{\psi}_n| = 2\sum_{(m,n)\in\hat{\mathcal{P}}_+} (\hat{\psi}_m - \hat{\psi}_n) \quad (21)$$

where the absolute value is trivial since $\hat{\phi}_{mn} \geq 0$ for all $(m,n) \in \mathcal{C}$.

Drawing similar relations on $\boldsymbol{\psi}'$, define the set $\mathcal{P}'_+ \subset \mathcal{C}$ containing any edge $(m,n) \in \mathcal{C}$ such that the flow ϕ'_{mn} is along the direction of $\mathbf{n}_\mathcal{C}$. Using the same argument as in (21) for $\boldsymbol{\psi}'$, we obtain

$$\sum_{(m,n)\in\mathcal{C}} |\psi'_m - \psi'_n| = 2 \sum_{(m,n)\in\mathcal{P}'_+} (\psi'_m - \psi'_n). \qquad (22)$$

Because the flows in $\hat{\boldsymbol{\phi}}$ for the edges in $\hat{\mathcal{P}}_+$ are aligned with $\mathbf{n}_\mathcal{C}$ and $\phi'_\ell > \hat{\phi}_\ell$ for these edges from (20), it follows that $\hat{\mathcal{P}}_+ \subseteq \mathcal{P}'_+$. Using the latter in (22), we get

$$2\sum_{(m,n)\in\hat{\mathcal{P}}_+} (\psi'_m - \psi'_n) \leq 2 \sum_{(m,n)\in\mathcal{P}'_+} (\psi'_m - \psi'_n)$$
$$= \sum_{(m,n)\in\mathcal{C}} |\psi'_m - \psi'_n|. \qquad (23)$$

For every edge $\ell = (m,n) \in \hat{\mathcal{P}}_+$, it holds that

$$\hat{\psi}_m - \hat{\psi}_n \overset{(a)}{=} a_\ell \hat{\phi}_\ell^2 \overset{(b)}{<} a_\ell \phi'^2_\ell \overset{(c)}{\leq} \psi'_m - \psi'_n \qquad (24)$$

where (a) comes from the definition of pressures in *Case 2* of Part II, (b) descends from $\phi'_\ell > \hat{\phi}_\ell > 0$, and (c) from (11). Summing (24) over all $\ell \in \hat{\mathcal{P}}_+$ and multiplying by 2 gives

$$2\sum_{(m,n)\in\hat{\mathcal{P}}_+} (\hat{\psi}_m - \hat{\psi}_n) < 2 \sum_{(m,n)\in\hat{\mathcal{P}}_+} (\psi'_m - \psi'_n)$$
$$\Rightarrow \sum_{(m,n)\in\mathcal{C}} |\hat{\psi}_m - \hat{\psi}_n| < \sum_{(m,n)\in\mathcal{C}} |\psi'_m - \psi'_n|$$

where the inequality stems from (22) and (23). From (19), the latter implies that $r(\boldsymbol{\psi}') > r(\hat{\boldsymbol{\psi}})$, hence contradicting the optimality of $\boldsymbol{\psi}'$. ∎

REFERENCES

[1] R. Z. Rios-Mercado and C. Borraz-Sanchez, "Optimization problems in natural gas transportation systems: A state-of-the-art review," *Appl. Energy*, vol. 147, pp. 536–555, Mar. 2015.

[2] "The future of natural gas: MIT energy initiative," Massachusetts Inst. Technology, Cambridge, MA, USA, Tech. Rep., 2011. [Online]. Available: http://energy.mit.edu/wp-content/uploads/2011/06/MITEI-The-Future-of-Natural-Gas.pdf

[3] A. Zlotnik, L. Roald, S. Backhaus, M. Chertkov, and G. Andersson, "Coordinated scheduling for interdependent electric power and natural gas infrastructures," *IEEE Trans. Power Syst.*, vol. 32, no. 1, pp. 600–610, Jan. 2017.

[4] C. Borraz-Sanchez, R. Bent, S. Backhaus, H. Hijazi, and P. V. Hentenryck, "Convex relaxations for gas expansion planning," *INFORMS J. Comput.*, vol. 28, no. 4, pp. 645–656, Aug. 2016.

[5] R. Bent, S. Blumsack, P. Van Hentenryck, C. Borraz-Sanchez, and M. Shahriari, "Joint electricity and natural gas transmission planning with endogenous market feedbacks," *IEEE Trans. Power Syst.*, vol. 33, no. 6, pp. 6397–6409, Nov. 2018.

[6] A. Zlotnik, M. Chertkov, and K. Turitsyn, "Assesing risk of gas-shortage in coupled gas-electricity infrastructures," in *Proc. Hawaii Int. Conf. Syst. Sci.*, Koloa, HI, USA, Jan. 2016, pp. 2519–2527.

[7] A. Schwele, C. Ordoudis, J. Kazempour, and P. Pinson, "Coordination of power and natural gas systems: Convexification approaches for linepack modeling," in *Proc. IEEE Power Energy Soc. PowerTech Conf.*, Milan, Italy, Jul. 2019, pp. 1–6.

[8] M. K. Singh and V. Kekatos, "Natural gas flow equations: Uniqueness and an MI-SOCP solver," in *Proc. IEEE Amer. Control Conf.*, Philadelphia, PA, USA, Jul. 2019, pp. 2114–2120.

[9] M. Vuffray, S. Misra, and M. Chertkov, "Monotonicity of dissipative flow networks renders robust maximum profit problem tractable: General analysis and application to natural gas flows," in *Proc. IEEE Conf. Decis. Control*, Osaka, Japan, Dec. 2015, pp. 4571–4578.

[10] A. Ojha, V. Kekatos, and R. Baldick, "Solving the natural gas flow problem using semidefinite program relaxation," in *Proc. IEEE Power Energy Soc. Gen. Meeting*, Chicago, IL, USA, Jul. 2017, pp. 1–5.

[11] A. Martinez-Mares and C. R. Fuerte-Esquivel, "A unified gas and power flow analysis in natural gas and electricity coupled networks," *IEEE Trans. Power Syst.*, vol. 27, no. 4, pp. 2156–2166, Nov. 2012.

[12] D. De Wolf and Y. Smeers, "The gas transmission problem solved by an extension of the simplex algorithm," *Manage. Sci.*, vol. 46, no. 11, pp. 1454–1465, Nov. 2000.

[13] S. Misra, M. Vuffray, and M. Chertkov, "Maximum throughput problem in dissipative flow networks with application to natural gas systems," 2015, *arXiv:1504.02370*.

[14] A. Osiadacz, *Simulation and Analysis of Gas Networks*. Houston, TX, USA: Gulf, 1987.

[15] A. Thorley and C. Tiley, "Unsteady and transient flow of compressible fluids in pipelines—A review of theoretical and some experimental studies," *Int. J. Heat Fluid Flow*, vol. 8, no. 1, pp. 3–15, Mar. 1987.

[16] S. Wu, L. R. Scott, and E. A. Boyd, "Towards the simplification of natural gas transmission networks," in *Proc. NSF Des. Manuf. Grantees Conf.*, Long Beach, CA, USA, Jan. 1999, pp. 26–41.

[17] Q. Li, S. An, and T. W. Gedra, "Solving natural gas loadflow problems using electric loadflow techniques," in *Proc. North Amer. Power Symp.*, Rolla, MO, USA, Oct. 2003, pp. 1–5.

[18] S. Misra, M. W. Fisher, S. Backhaus, R. Bent, M. Chertkov, and F. Pan, "Optimal compression in natural gas networks: A geometric programming approach," *IEEE Trans. Control Netw. Syst.*, vol. 2, no. 1, pp. 47–56, Mar. 2015.

[19] M. K. Singh and V. Kekatos, "On the flow problem in water distribution networks: Uniqueness and solvers," Feb. 2019, *arXiv:1901.03676*.

[20] M. K. Singh and V. Kekatos, "Optimal scheduling of water distribution systems," *IEEE Trans. Control Netw. Syst.*, to be published.

[21] G. P. McCormick, "Computability of global solutions to factorable nonconvex programs: Part I—Convex underestimating problems," *Math. Program.*, vol. 10, no. 1, pp. 147–175, Dec. 1976.

[22] C. B. Sanchez, R. Bent, S. Backhaus, S. Blumsack, H. Hijazi, and P. van Hentenryck, "Convex optimization for joint expansion planning of natural gas and power systems," in *Proc. Hawaii Int. Conf. Syst. Sci.*, Koloa, HI, USA, Jan. 2016, pp. 2536–2545.

[23] T. Ding, Y. Xu, Y. Yang, Z. Li, X. Zhang, and F. Blaabjerg, "A tight linear program for feasibility check and solutions to natural gas flow equations," *IEEE Trans. Power Syst.*, vol. 34, no. 3, pp. 2441–2444, May 2019.

[24] D. Assmann, F. Liers, and M. Stingl, "Decomposable robust two-stage optimization: An application to gas network operations under uncertainty," *Networks*, vol. 74, pp. 40–61, Jul. 2019.

[25] P. Benner, S. Grundel, C. Himpe, C. Huck, T. Streubel, and C. Tischendorf, "Gas network benchmark models, " in, *Differential-Algebraic Equations Forum*. Heidelberg, Germany: Springer, 2018.

[26] S. Chen, Z. Wei, G. Sun, D. Wang, and H. Zang, "Steady state and transient simulation for electricity-gas integrated energy systems by using convex optimisation," *IET Gen., Transm. Distrib.*, vol. 12, no. 9, pp. 2199–2206, May 2018.

[27] M. Zholbaryssov and A. D. Dominguez-Garcia, "Convex relaxations of the network flow problem under cycle constraints," *IEEE Trans. Control Netw. Syst.*, to be published, doi: 10.1109/TCNS.2019.2915390.

[28] J. Lofberg, "YALMIP: A toolbox for modeling and optimization in MATLAB," in *Proc IEEE Int. Conf. Robot. Autom.*, New Orleans, LA, USA, Sep. 2004, pp. 284–289.

[29] IBM Corporation, "IBM ILOG CPLEX Optimization Studio CPLEX user's manual," 2017. [Online]. Available: http://www.ibm.com

[30] M. Schmidt *et al.*, "Gaslib—A library of gas network instances," *Data*, vol. 2, no. 40, pp. 1–18, 2017.

[31] B. Korte and J. Vygen, *Combinatorial Optimization*, vol. 2. Heidelberg, Germany: Springer, 2012.

[32] C. Godsil and G. Royle, *Algebraic Graph Theory*. New York, NY, USA: Springer, 2001.

Manish Kumar Singh (Student Member, IEEE) received the B.Tech. degree in electrical engineering from the Indian Institute of Technology (BHU), Varanasi, India, in 2013, and the M.S. degree in electrical engineering from Virginia Tech, Blacksburg, VA, USA, in 2018, where he is currently working toward the Ph.D. degree in electrical engineering.

From 2013 to 2016, he was an Engineer with the Smart Grid Department of POWERGRID, the central transmission utility of India. His current research focuses on the application of optimization, control, and graph-theoretic techniques to develop algorithmic solutions for operation and analysis of water, natural gas, and electric power systems.

Vassilis Kekatos (Senior Member, IEEE) received the Diploma, M.Sc., and Ph.D. degrees in computer science and computer engineering from the University of Patras, Patras, Greece, in 2001, 2003, and 2007, respectively.

He is currently an Assistant Professor with the Bradley Department of Electrical and Computer Engineering (ECE), Virginia Tech, Blacksburg, VA, USA. He has been a Research Associate with the ECE Department, University of Minnesota, Minneapolis, MN, USA. In 2014, he was with the University of Texas at Austin and Ohio State University, Columbus, OH, USA, as a Visiting Researcher. His current research focuses on the optimization and learning for future energy systems.

Dr. Kekatos is a recipient of the NSF Career Award in 2018 and the Marie Curie Fellowship. He is also a recipient of the Postdoctoral Career Development Award (honorable mention) at the University of Minnesota. He is currently an editorial board member for the IEEE TRANSACTIONS ON SMART GRID.